Available online at www.eccomasproceedia.org
Eccomas Proceedia SMART (2023) 1100-1112

ECCOMAS
Proceedia

X ECCOMAS Thematic Conference on Smart Structures and Materials
SMART 2023
D.A. Saravanos, A. Benjeddou, N. Chrysochoidis and T. Theodosiou (Eds)

REMOVAL OF EFFECTS FROM PERODIC EXCITATION ON OPERATIONAL MODAL ANALYSIS USING SPECTRAL KURTOSIS AND FOURIER SERIES

MARCEL WIEMANN*, LUKAS BONEKEMPER* AND PETER KRAEMER*

* Chair of Mechanics with a focus on Structural Health Monitoring, (MSHM)
University of Siegen
Campus Paul Bonatz, 57076 Siegen, Germany
e-mail: marcel.wiemann@uni-siegen.de, www.uni-siegen.de

Abstract. The modal analysis belongs to the elementary diagnostic tools for monitoring and damage analysis of structures or individual mechanical structural components coupled with rotating machine parts. For vibration-based damage diagnosis and continuous monitoring of modal quantities, different operational modal analysis (OMA) approaches in time domain are known. In most cases the results of the analysis (modal data) are improved with help of post-processing methods e.g., by clustering of stable poles in stability diagrams. The purpose of this paper is to facilitate the automatic interpretability of the calculation results through data pre-processing. The method presented in this paper is used to remove unwanted signal components to identify natural frequencies more accurately. To achieve this goal, algorithms based on the Fourier Series are applied for the cancelation of rotational speed related frequencies and their harmonics, which can have a negative effect on the estimation of the eigenfrequencies and the associated damping, especially if the interfering frequencies are close to an eigenfrequency. The improved eigenfrequency identification within the Covariance-Driven Stochastic Subspace Identification (COV-SSI) is performed after a comparative analysis of the signal energies and properties in the effected frequency bands by using the Power Spectral Density (PSD) and the Spectral Kurtosis. This helps to identify signal components from the periodic excitation and to guarantee that only those are removed. Afterwards, the mentioned pre-processing approach will be used together with well-known post-processing methods (e.g., stability plot cleansing by help of clustering). The effectiveness of the pre-processing approach is examined by means of simulated acceleration signals of a 3-DOF-Mass-spring-damper system in state space. The advantages and the limitations of the methods as well as the future work based on the presented methodology will be discussed.

Key words: Operational Modal Analysis, Covariance Driven Stochastic Subspace Identification, Spectral Kurtosis, Fourier Series, Removal of Harmonics.

1 INTRODUCTION

The Operational Modal Analysis is a widely used method for system identification in the area of Structural Health Monitoring (SHM). It could identify eigenfrequencies of a structure,

Peer-review under responsibility of the organizing committee of SMART 2023.
doi: 10.7712/150123.9860.450314

damping values and the corresponding mode shapes. There are different techniques which can be used for the estimation of the wanted parameters such as SSI-Data, Peak Picking, Polymax. Each of them has its own advantages and disadvantages [1, 2]. This paper only deals with the SSI-COV algorithm. But in general, the preprocessing steps should be applicable for other OMA methods or even other use cases [3]. The operational modal analysis can be used from theoretical point of view, in case of stochastic excitation, e.g., when the structure is excited by ambient loads, for example wind, traffic or waves. But in practice OMA is often applied to calculate the dynamical properties of load-bearing structures for machines. In this case the structure is excited by rotational related frequencies e.g., from pumps, generators or gearboxes and the rotational frequencies are a part of the overall excitation. Depending on the structure, the amplitude of the harmonic loads in various frequency bands and the position of the acceleration sensors can have a large contribution to the response spectrum. This in turn can have a negative effect on the stability diagram and its interpretability and therefore on the results in general [4–6]. In the following chapters an approach is presented which is used to minimize the negative effects of rotation related frequencies by using the Spectral Kurtosis (SK) to identify, and the Fourier Series (FS) to remove these frequencies. The approach in this work was developed as part of an automated OMA to be used in context of SHM [7, 8]. The underlying idea is to remove interfering signal components in the measurement data before the actual SSI-COV algorithm is applied.

2 FUNDAMENTALS OF SSI-COV

The following chapter gives a brief overview of the SSI-COV algorithm so that the effects of the herein proposed methods can be better comprehended. A more detailed explanation can be found in the publication by Rainieri and Fabbrochino [2]. The algorithm belongs to the output-only methods for system identification, originally based on the eigenvalue realization algorithm designed for known impulse excitation [9]. In case of SSI-COV the structure response is “modeled” as a state-space model and the unknown excitation is assumed to be uniformly distributed white noise. In practice the amplitude or the excitation distribution is unknown, which means that modes in various frequency bands can be stimulated differently. That can make a reliable system identification quite difficult. Precisely because the derivation assumes a stochastic excitation. The following equations and relations of the State Space System are applied:

State space equation (1)

Measurement equation (2)

Output covariance matrix [ ] (3)

State output covariance matrix = [ ] (4)

It is assumed that all relevant variables are not correlated and independent of each other excluding the initial covariance and the initial state. Multiplying the measured data with the measurement equation Eq. (2) under consideration of Eq. (3)-Eq. (4) leads to the following relationship in Eq. (5)

Output covariance (5)

The results from the cross and auto covariance functions between the sensor signals are arranged in a block Hankel matrix Eq. (6). The index variable i from Equation (5) corresponds to the time steps of the correlation function.

$$\begin{bmatrix} & & \cdots & \\ \vdots & \vdots & \ddots & \vdots \\ & & & \end{bmatrix} \tag{6}$$

To extract the modal parameters, it is necessary to decompose the m x m Hankel matrix into a unitary U, into an adjoint V and into a diagonal matrix S by use of the Singular Value Decomposition (SVD). The dimension can be obtained as given by Eq. (7).

$$m = number\ of\ sensors \cdot max(i) / 2 \tag{7}$$

The dimension of the Hankel matrix determines the maximum model order and has a significant influence on the true information content. Weakly excited modes can only be detected by a higher model order and consequently a high dimension Hankel matrix. The drawback is that the stability diagram will also contain more spurious or mathematical poles. The system matrix A_d can be now obtained by the Eq. (8).

System matrix . . . . (8)

The index p is equivalent to the actual model order and represents a dimensional reduction of the matrices U, S and V, which are estimated using SVD.

$$\begin{bmatrix} & \cdots & \\ \vdots & \ddots & \vdots \\ & \cdots & \end{bmatrix} \quad \begin{bmatrix} & \cdots & \\ \vdots & \ddots & \vdots \\ & \cdots & \end{bmatrix} \quad \begin{bmatrix} & \cdots & \\ \vdots & \ddots & \vdots \\ & \cdots & \end{bmatrix} \tag{9}$$

Hereby the calculation of A_d in Eq. (8) is repeated from the maximum fixed order to the minimum order under the assumption that stable modes are reproduced in most of the calculation orders. The SVD is only performed once for the highest model order.

3 INTRODUCTIONS OF 3DOF STATE SPACE MODEL

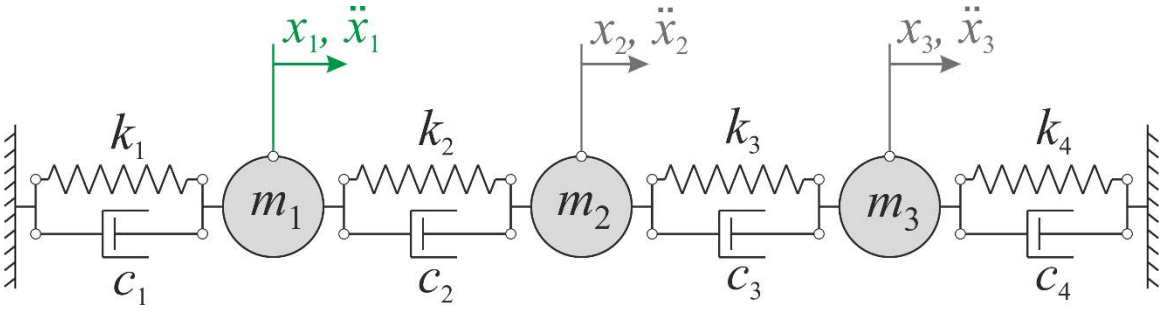

Figure 1: 3-DOF mass-spring-damper model

To evaluate the approaches a 3-DOF-Model (see Figure 1) is transformed in a state space system. This allows to vary the excitation, damping, natural frequencies and external influences as needed to check the general suitability of the methods. This simple simulation ensures that all the necessary assumptions of SSI-COV e.g., Eq. 3 and 4 can be fulfilled. Furthermore, it can be said in this context that methods that do not lead to the desired result by means of simulations rarely achieve better results in real measurements. The excitation is induced at mass m1 as displacement x1. The system response (¨ ¨ ¨ is used as m-variate time series as input for the Spectral Kurtosis and the subsequent removal process with help of the FS. As described above, for the detection of eigenfrequencies by SSI-COV it is assumed, that the excitation is a uniformly distributed white noise. For real existing structures this case rarely exists. Instead, the distribution of the excitation is widely unknown or polluted by harmonic components. That makes the identification of eigenfrequencies complicated because sometimes these are not or only excited by natural loads. The identification is more complex in the case that these are excited by harmonic input. To evaluate our approach for removal of unwanted spectral signal components, different ratios between the stochastic and harmonic excitation, are used. In the following the variable *r* shows this proportion. ^ describes the general maximum amplitude for the stochastic part of the signal and the continuous amplitude of the rotational related frequencies which are induced as sine wave.

Excitation ratio $\frac{\hat{}}{\hat{}}$ (8)

It can be observed that, contrary to the expectation, a strong harmonic excitation does not necessarily have a major negative influence on the results of the modal analysis, but that even relatively small harmonic amplitudes lead to a poorer interpretability of the stability diagram. The reason for that could be, that the SSI-COV algorithm can separate a strong harmonic excitation better than a low one which blurred the structural response. For this purpose, simulated tests are conducted for different excitation ratios. The eigenfrequencies of the 3-DOF-Model are 31.72 Hz, 49.77 Hz and 64.48 Hz, the frequencies of the harmonic excitations are 50Hz, 75Hz and 100Hz.

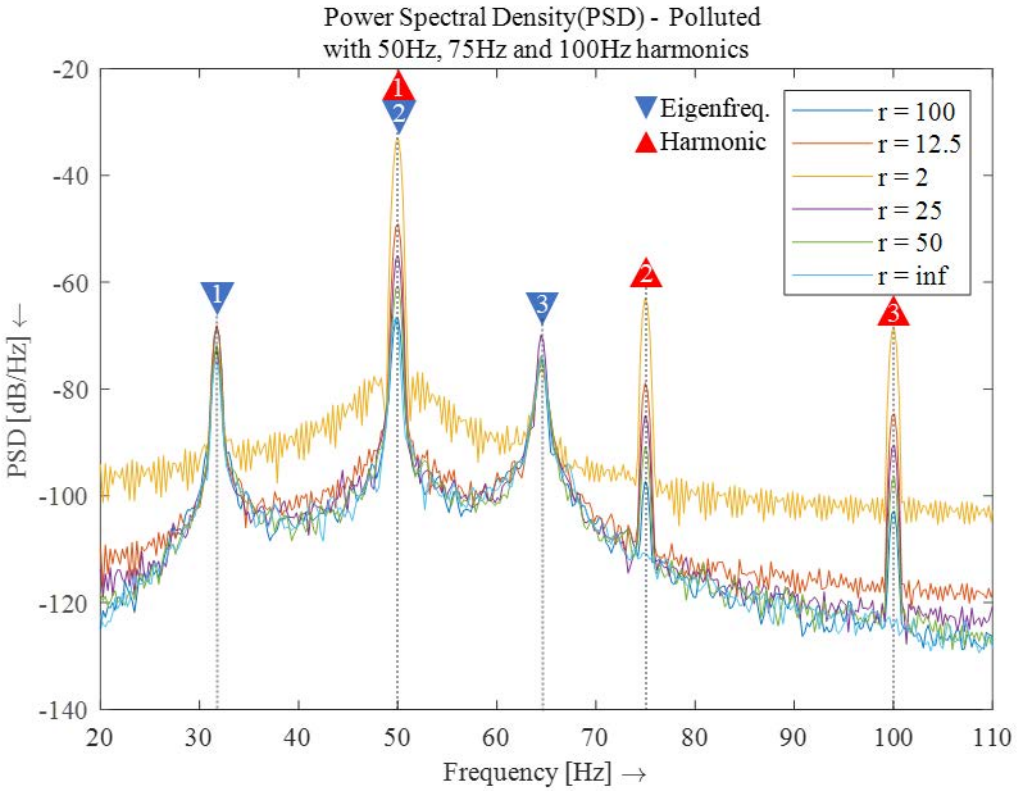

Figure 2: Response spectrum of the three-mass-spring-damper oscillator with harmonic excitation

Figure 2 shows a strong excitation of the second natural frequency by the harmonic of 50 Hz. Depending on the excitation ratio, the peak in the spectrum shifts and makes a reliable detection of the second eigenfrequency difficult.

4 DETECTION OF HARMONIC COMPONENTS

There are many methods for identifying harmonic signal components, a well-known method is the Spectral Kurtosis, which is also used here. [10, 11] It is a statistical tool that detects the presence of transient components in the signal and can determine their position in the frequency band. There are numerous further developments of the Spectral Kurtosis (SK) to facilitate the detection of harmonic signal components, but in this case the well-known calculation procedure for determining the Spectral Kurtosis is applied with sufficient accuracy [5, 12].

Spectral Kurtosis $\qquad \_\_\_\_ \cdot \left[\frac{\cdot \Sigma_i}{\left(\Sigma_i \qquad \right)} \right]$ (10)

Reliable detection of harmonic signal components is essential for subsequent removal of interfering components. Using Spectral Kurtosis, the interfering harmonic signal components of the simulation can be identified and provide the fundamental harmonic for subsequent removal using the Fourier Series. It must be added that an accurate estimation of harmonic

components strongly depends on the signal properties and the used settings for the Spectral Kurtosis. is the Fourier transformed signal and the number of windows. A change of or of the parameters to estimate will directly influence the estimation results of the SK. indicates a non-stationary signal, a stationary normally distributed part and -1 a stationary harmonic component.

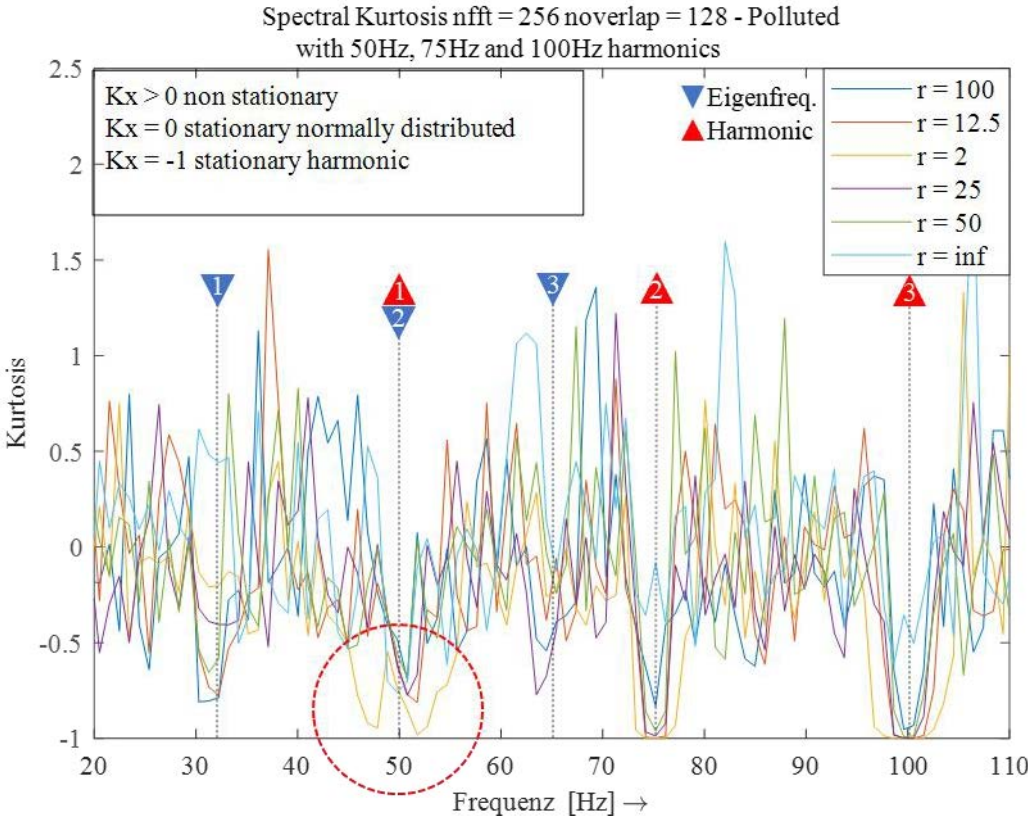

Figure 3: Spectral Kurtosis of the response signal of the three-mass oscillator

Figure 3 shows the results of the SK of the acceleration of mass one and clearly demonstrates the influence of the three harmonic components on the SK curve. Due to the superposition of the natural frequency with the harmonic at 50Hz, an abnormal splitting of the SK curve occurs with a strong uniform excitation for ratio r=2 (Red circle). Depending on the position in the frequency band a possible overlay with an existing natural frequency can make a precise determination of the fundamental harmonics difficult. Since the general purpose here is to present the feasibility and not the automated algorithm, no threshold has been set for Kx to decide if the signal component is stationary harmonic or stationary normally distributed. The settings to calculate the SK, are shown in the title of the diagram. The obtained outcome of the Spectral Kurtosis is then used as input for the following removal process.

5 DISCRETE FOURIER SERIES FOR FREQUENCY REMOVAL

To remove the interfering harmonic signal components, the Fourier Series (FS) for harmonic signal reconstruction with subsequent subtraction from the original signal is used. To do this, the detected fundamental harmonic from the system response is used for ω_0. The number of

Fourier coefficients can be largely determined from the results of the SK and the associated number of higher harmonics. The assumption is made that the signal to be reconstructed is a periodic function (Eq .11).

$$( ) \tag{11}$$

Therefore, it can be described by the following Fourier Series as basic formula. (Eq .12). k corresponds to the number of Fourier coefficients and thus also to the number of harmonics to be removed.

$$( ) - \sum \quad (\quad) \quad (\quad) \tag{12}$$

The coefficients b_n, a_n and a_0 are calculated as follows. Eq. 13, Eq.14 and Eq.15. (Left continuous), (Right discrete)

$$-\int \quad ( ) \cdot \quad (\cdot \quad \cdot) \cdot \qquad \_ \cdot \sum \cdot \quad \cdot \quad \cdot \tag{13}$$

$$-\int \quad ( ) \cdot \quad (\cdot \quad \cdot) \cdot \qquad \_ \cdot \sum \cdot \quad \cdot \quad \cdot \tag{14}$$

$$-\int \quad ( ) \cdot \qquad \_ \cdot \sum \tag{15}$$

The reconstructed discrete signal $h(t)$ in this way maps the harmonic signal components which are present in the response spectrum $(\ddot{x}_1, \ddot{x}_2, \ddot{x}_3)$ and thus allows them to be removed from the discrete signal $\ddot{x}(t)$ by subtraction, which then deletes the unwanted frequency components. ( ) is then used as input for the modal analysis respectively as .

$$y_{rec}(t) = \ddot{x}(t) - h(t) \tag{16}$$

The signal is generally attenuated by the clean-up. Natural frequencies that lie in the range of the interference frequencies are not affected by the removal and can therefore still be detected and calculated via the modal analysis. Ultimately, the calculation must be done separately for each channel, as this is the only way to achieve precise results. An individual adjustment for ω_0 and the coefficients is therefore necessary.

5.1 Removal interval for an iterated calculation

Even if the disturbing harmonic frequency could not be identified exactly for example when the spectral resolution was not high enough, a frequency interval for ω_0 could be used. In this case the removal process needs to be repeated for each discrete element in the according frequency interval. If the interval is selected “correctly” the procedure has not a negative influence on the signal. If the interval is chosen too generously, not only the harmonic part is removed. An example with a simple signal shows the behavior. The signal consists of noise and two harmonic components at 30 Hz and 46,77 Hz, which was randomly selected. A second fundamental harmonic is used in this example to show that only the selected

fundamental is explicitly removed. Figure 4 left illustrate the results by using a small interval Hz and on the right by using a quite large interval 28 Hz. As a side aspect and for comparison the diagram also shows what happened when a notch filter is used instead. It can be observed that the small interval just removes the harmonic disturbance and attempts to remove the inexistent second harmonic of the first fundamental harmonic (30 Hz). Overall, the iterated calculation with the small interval does not affect the rest of the signal significantly. However, when the large interval for is used the impact on the signal is much larger and leads to suppression of frequencies which are not related to the harmonic components. Compared to the use of a notch filter, the power of the cleaned signal in the corresponding frequency band is only reduced to an average level of the surrounding frequencies. A more significant suppression does not happen if the interval is narrow around the harmonic component.

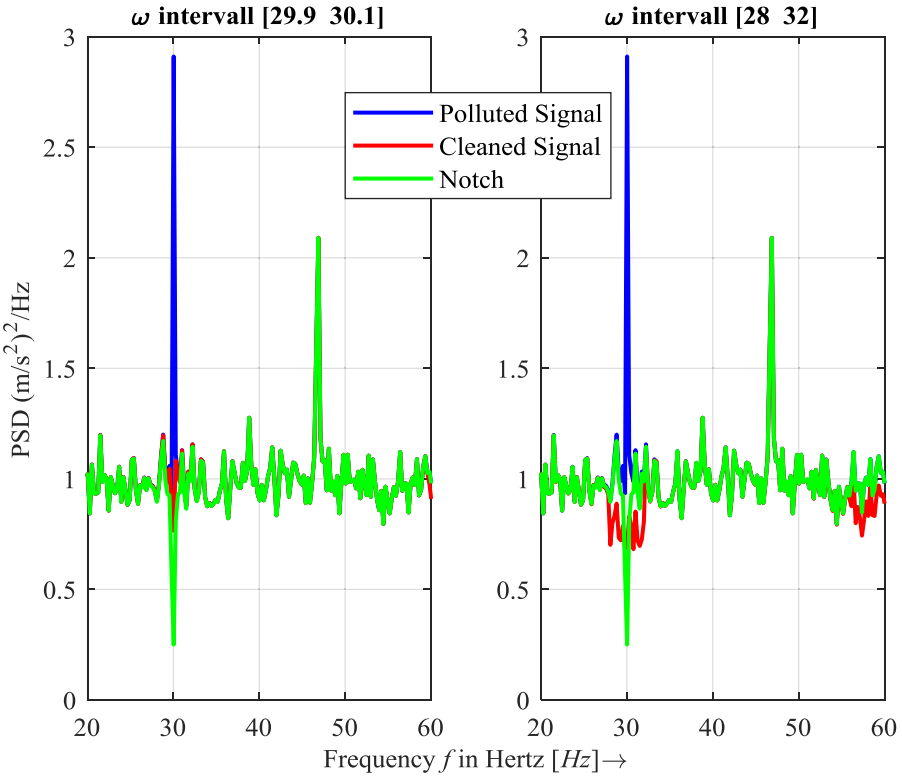

Figure 4: Use of $_0$ intervals of different sizes - influence on the removal

5.2 Signal properties after removing of harmonic components

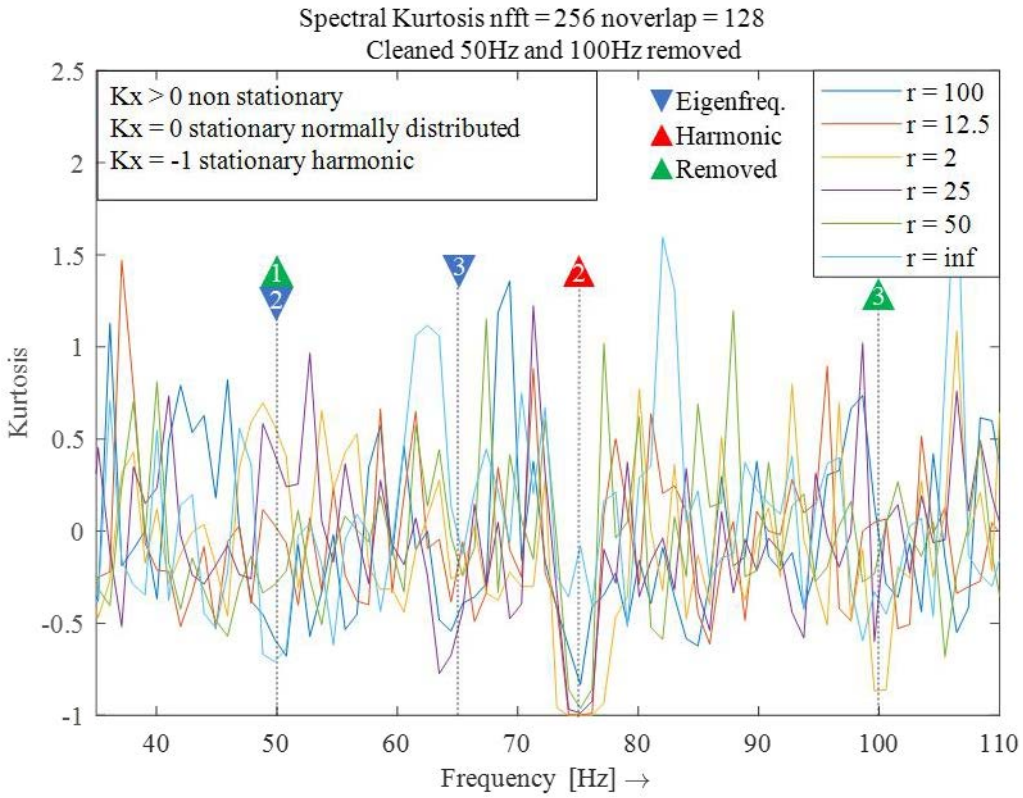

Figure 5: Spectral Kurtosis of the adjusted response signal of the three-mass oscillator

Figure 5 shows the signal without the two adjusted harmonic components. Here, 50 Hz was chosen as the fundamental harmonic and two coefficients as input parameters. Compared to Figure 3, the signal change in the corresponding frequency ranges can be clearly seen. The additional harmonic component at 75 Hz remains just as unaffected as the other frequency bands regarding their signal characteristics. If the harmonic excitation is large in relation to the noise excitation (r=2 in Figure 5), the second harmonic at 100 Hz cannot be completely removed. This can also be seen well in the frequency spectrum. With regard to the second natural frequency, which was strongly influenced by the excitation, it is easy to see that a backshift of the peak has taken place, which facilitates the reliable detection by the modal analysis, see Figure 6. Due to the strong harmonic component the peak of the eigenfrequency was widened and shifted to the frequency of the harmonic (50 Hz). A further comparison of the PSD (Figure 2 to Figure 6) shows that the frequency band of around 50 Hz lose a significant amount of energy through the removal of the harmonic component (10dB). Around 100Hz the PSD curve shows values which could give the impression that there was no harmonic distortion. The frequency curve of the cleaned signal fits now relatively well with the surrounding spectrum.

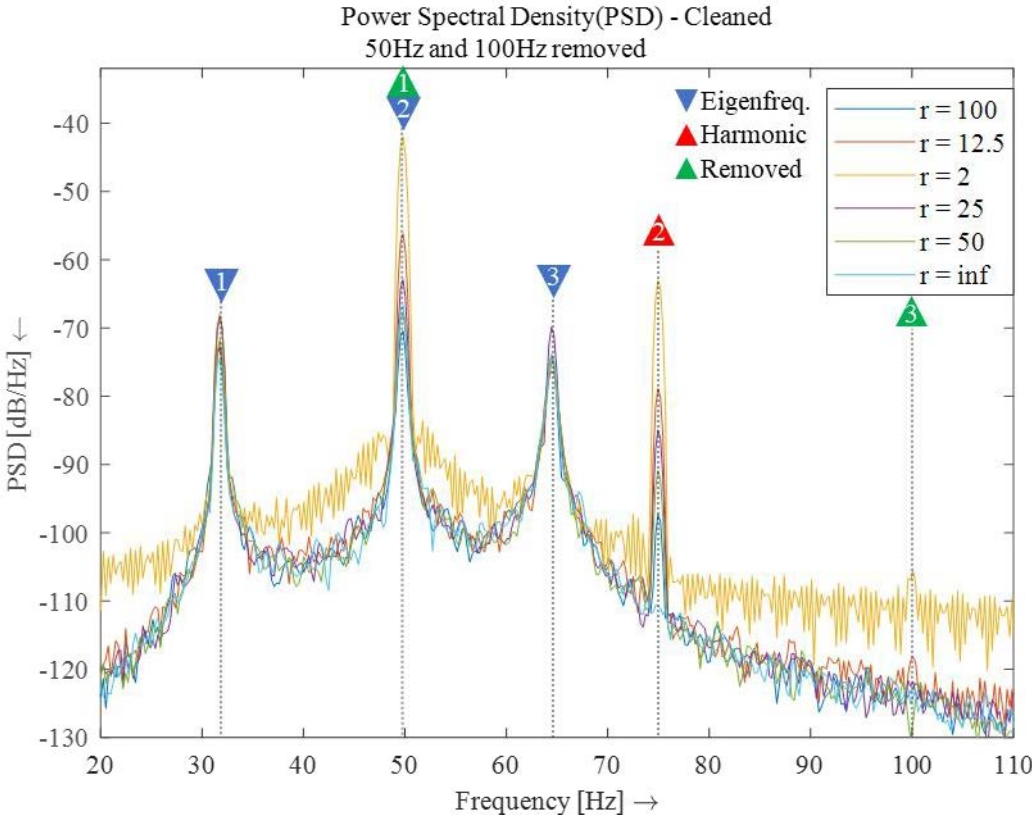

Figure 6: Response spectrum of the three-mass oscillator without harmonic excitation at 50Hz and 100Hz

6 IMPACTS ON OPERATIONAL MODAL ANALYSIS

To check the efficiency of the algorithm, the modal parameters of the system are now determined as described in chapter two. The model order is chosen untypically high for such a system and only serves to better visualize the result. After the poles have been calculated, clustering is carried out using the criteria in [8]. Figure 7 shows the result of the modal analysis with the contaminated acceleration signals. The harmonic excitation frequencies are clearly recognized as poles by the SSI-COV algorithm and visually exhibit all the characteristics of a stable natural frequency. All poles marked in grey are interpreted as either mathematical poles or harmonic signal components. Due to the proximity to the harmonic excitation of 50 Hz, the cluster algorithm is not able to assign the poles to the stable natural frequency (49.77 Hz). In this example, the remaining harmonic frequencies are not identified as eigenfrequencies, which in turn is due to the low permitted percentage damping deviation, which in the case of already low damping values allows almost no absolute deviation. The standard deviation of the third eigenfrequency at 64,48 Hz is high compared to the first natural frequency, this is not only due to the harmonic components in the excitation signal, but also due to the relatively small overall excitation which is introduced at mass one. A higher excitation amplitude for $\hat{A}_{noise}$ or if the excitation is introduced at all masses of the system, would reduce the standard deviation.

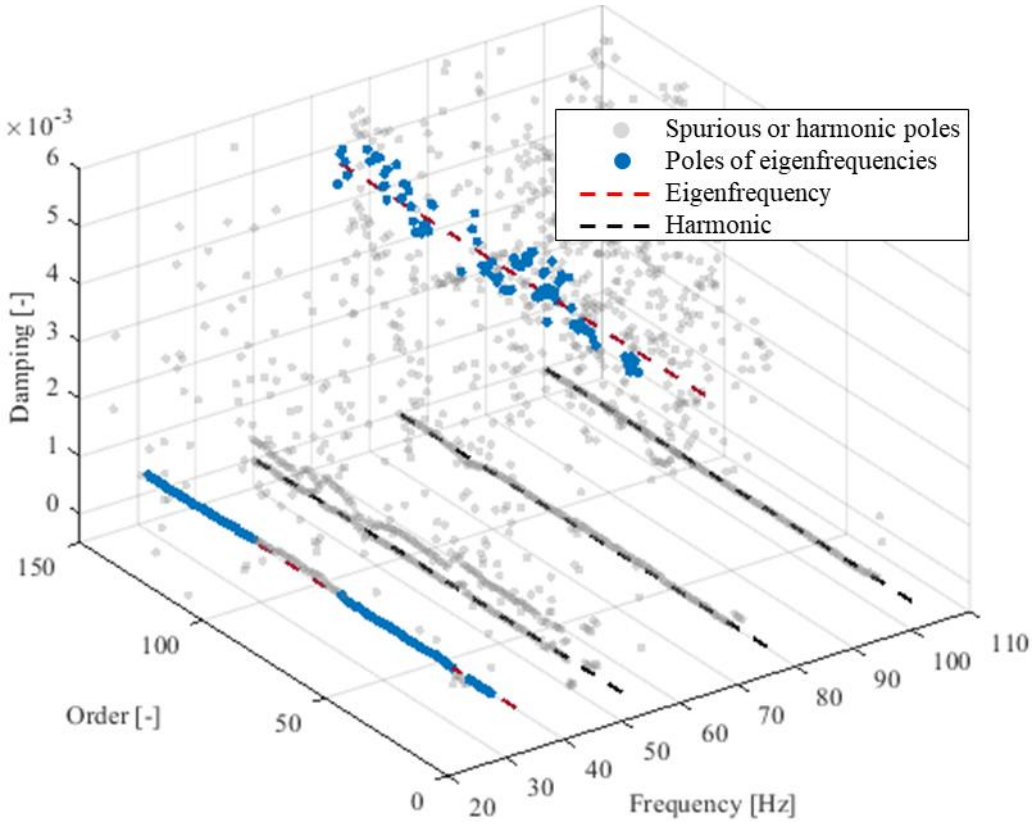

Figure 7: Three-dimensional stability diagram as result of the OMA with harmonic components at 50, 75 and 100Hz and excitation ratio r=100

Figure 8 shows the results after the removal of the harmonic components, the cluster algorithm is now able to detect the second eigenfrequency with a sufficient accuracy. The removal of the harmonic components facilitates the detection of eigenfrequencies by the cluster algorithm because poles caused by the harmonics are removed and therefore are no longer potentially associated to a cluster. Another positive aspect is that the scattering of the poles of the second eigenfrequency (very closed to the harmonic by 50Hz) could be reduced, so that the results for frequency and damping are accurate. The determined frequency of the first natural frequency has slightly deteriorated, but here we also speak of a deviation in the range of 10^{-3} Hz. Beside this, the estimation of the third eigenfrequency and the damping values of all eigenfrequencies could be improved. Also, the standard deviation of the clusters could be reduced by removing the harmonics. The stabilization diagram shows no indication of the presence of the first fundamental harmonic (50Hz) and the related harmonic at 100 Hz. The second fundamental harmonic at 75 Hz, remains unaffected by the removal process because of the selection of 50 Hz as base frequency for the Fourier Series even if the number of coefficients would be increased. If there is a need to remove also the second fundamental harmonic and the belonging higher harmonics, the removal process must be repeated with 75Hz as base frequency for the Fourier Series. However, at this stage it is recommended to remove only the frequencies that interfere with the modal analysis.

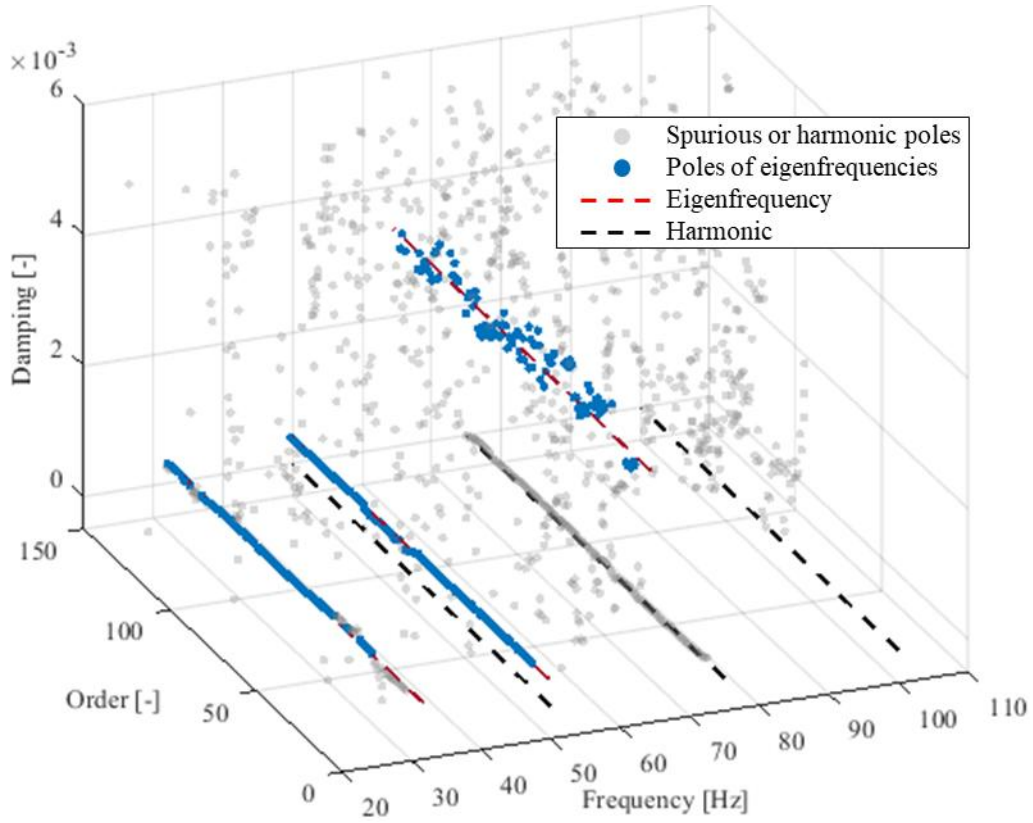

Figure 8: Three-dimensional stability diagram as result of the OMA with removed harmonic components (50 Hz and 100 Hz) and excitation ratio r=100

6 LIMITATIONS AND ADVANTAGES OF THE CHOSEN APPROACH AND PERSPECTIVES FOR FURTHER RESEARCH

The approach shown here was successfully evaluated on simulated data. A removal of interfering harmonics can facilitate the clustering process of the calculated poles thus less poles are sorted to a cluster of a potential eigenfrequency. Also, the scattering of poles which belongs to an eigenfrequency nearby a harmonic disturbance could be reduced. This in turn shows that a harmonic could have a direct negative impact on the SSI-COV algorithm. Significant for the success of the proposed approach is a robust and reliable detection of the fundamental harmonics via the Spectral Kurtosis. Unfortunately, the estimation of the harmonic components is not straightforward although the Spectral Kurtosis is a well-known signal processing method. The results strongly depend on the variance of the harmonic frequency. Due to this, however, the influence of errors in the detection of the first fundamental harmonic and its variation must also be investigated in future work. This means that the method will have to be further optimized for application to real measurement data from structures in-situ. By varying the excitation ratio, it was also possible to show that if a harmonic can be well removed, depends on its amplitude. Also, it cannot be generalized that a stronger harmonic excitation leads directly to worse results of the modal analysis.

ACKNOWLEDGEMENT

The authors gratefully acknowledge the financial support of this research by the German Federal Ministry for Economic Affairs and Energy (grant number 03EE3023B, Project In-Situ Wind).

References

[1] J.-H. Yi and C.-B Yun "Comparative study on modal identi ication methods using output-only in ormation " *Structural Engineering and Mechanics*, vol. 17, 3_4, pp. 445–466, 2004, doi: 10.12989/sem.2004.17.3_4.445.

[2] C. Rainieri and G. Fabbrocino, *Operational Modal Analysis of Civil Engineering Structures*. New York, NY: Springer New York, 2014.

[3] M Bahaz and R Benzid " icient algorithm or baseline wander and powerline noise removal rom C G signals based on discrete Fourier series " *Australasian physical & engineering sciences in medicine*, early access. doi: 10.1007/s13246-018-0623-1.

[4] S Gres P Andersen C Hoen and L Damkilde "Orthogonal Projection-Based Harmonic Signal Removal or Operational Modal Analysis " in *Structural Health Monitoring, Photogrammetry & DIC, Volume 6* (Conference Proceedings of the Society for Experimental Mechanics Series), C. Niezrecki and J. Baqersad, Eds., Cham: Springer International Publishing, 2019, pp. 9–21.

[5] J.-L Dion I Taw iq and G Chevallier "Harmonic component detection: Optimized Spectral ur tosis or operational modal analysis " *Mechanical Systems and Signal Processing*, vol. 26, no. 2, pp. 24–33, 2012, doi: 10.1016/j.ymssp.2011.07.009.

[6] Z Xia T Wang and L Zhang "Detection and removal o harmonic components in operational modal analysis " *J VIBROENG*, vol. 19, no. 7, pp. 5278–5289, 2017, doi: 10.21595/jve.2017.17725.

[7] M Wiemann L Bonekemper and P r aemer "Methods to enhance the automation of operational modal analysis " *Vib. proced.*, vol. 31, pp. 46–51, 2020, doi: 10.21595/vp.2020.21443.

[8] L Bonekemper M Wiemann and P r aemer "Automated set-up parameter estimation and result evaluation for SSI-Cov-OMA " *Vib. proced.*, vol. 34, pp. 43–49, 2020, doi: 10.21595/vp.2020.21742.

[9] R Ho BL " ective construction o linear state-variable models from input/ output data " *Regelungstechnik*, pp. 545–548, 1966.

[10] J Antoni "The spectral kurtosis: a use ul tool for characterising non-stationary signals " *Mechanical Systems and Signal Processing*, vol. 20, no. 2, pp. 282–307, 2006, doi: 10.1016/j.ymssp.2004.09.001.

[11] J Antoni and R B Randall "The spectral kurtosis: application to the vibratory surveillance and diagnostics o rotating machines " *Mechanical Systems and Signal Processing*, vol. 20, no. 2, pp. 308–331, 2006, doi: 10.1016/j.ymssp.2004.09.002.

[12] N Sawalhi R B Randall and H ndo " The enhancement o ault detection and diagnosis in rolling element bearings using minimum entropy deconvolution combined with spectral kurtosis " *Mechanical Systems and Signal Processing*, vol. 21, no. 6, pp. 2616–2633, 2007, doi: 10.1016/j.ymssp.2006.12.002.